

Detection of Low Resistivity Reservoirs Using GR Spectrometry Logs: A Case Study*

Xia Zhu¹, Ling Yun¹, Guo Jianming¹, Zhang Sheng¹, Xu Hai¹, Zhang Tingting¹, Zhao Shiquan¹, Bie Jing¹, and Li Kai¹

Search and Discovery Article #41350 (2014)

Posted May 12, 2014

*Adapted from extended abstract prepared in conjunction with poster presentation at GEO-2014, 11th Middle East Geosciences Conference and Exhibition, 10-12 March 2014, GEO-2014©2014

¹BGP, CNPC, Beijing, China

Abstract

The oilfield a-13-2 is located in the C - low uplift of X Basin in south China. In this oilfield, the Enping and Zhuhai Formations of Paleogene at well L13-2-1 were interpreted as oil - water-bearing layers using the conventional well logging data. However, the sidewall core data indicate that these formations are oil - bearing reservoir. It is challenging to determine whether these formations are oil - water bearing or oil bearing with low resistivity due to the sparsity of the wells and the lack of the necessary test on the core data, which may accurately discriminate the reservoir type, evaluate the reservoir and enhance the oil recovery in the oilfield. In this paper, the core samples from the zones of interest in this oilfield and the adjacent one (the oilfield b-13-1 and B-depression) were analyzed, and the diagenetic geology are studied. Afterwards, using the cross - plot and histogram of the TH and K from the gamma ray spectrometry logs, the clay mineral type with high adsorbing water, mass fraction and the low - resistivity mechanism caused by the conductive water - film net of the clay mineral were studied. Based on our study, the following new conclusions have been drawn on the water-oil bearing formations at well L13-2-1: the zone in depth from 2,879.5 meters to 2,885 meters that was considered as oil - water formations is actually the oil layers with rich bound water and low resistivity.

Introduction

The study area, a-13-2 oilfield, is located in the Zhuyi depression – C-low uplift of north depression in south China basin. The basin developed through taphrogenesis, with depression and block uplift in the Cenozoic era ([Figure 1](#)). Cores from the Enping Formation (depth from 2,879.5m to 2,885m) in well L13-2-1 are continental fine sandstone, with low resistivity ($<2 \Omega \cdot m$), low GR, low density and resistivity and ratio of oil saturated layer to water saturated layer less than 2.3 on log data. The Enping Formation is interpreted as oil-water layer by conventional logging interpretation, but it is rich oil layer from cores ([Figure 2](#)). Due to a few drilling wells and lack of core analysis, it is hard to judge whether the reservoir type is oil-water bearing layers or low resistivity oil layers by only log data. Some papers (Liao et al, 2010; Hu et al, 2010; Fu, 2000; Zou et al, 2007) reported that low resistivity oil layers exist in Zhujiang (Neogene) and Zhuhai (Paleogene) Formations in this area and b-13-1 oilfield, but there is no report of low resistivity oil layers in Enping Formation. Low resistivity oil layers are complex. By detailed analysis and research of log data in the study area, we discovered that major factors of low resistivity oil layers are the especial diagenetic environment and high-irreducible water clay minerals in pores. Based on petrological characteristics, diagenetic environment and

physical properties of low resistivity formations, clay characteristics of sand reservoir in well L13-2-1 and well F13-1-1 are studied and analyzed using cross-plot and histogram of TH and K in GR spectrum log. Then the deep oil-water layers in well L13-2-1 are reinterpreted and the mechanism of low resistivity layers is preliminarily discussed.

Basic Characteristics of Low Resistivity Reservoirs

Sand reservoirs of the Enping and Zhuhai formations show low composition maturity and low structure maturity with near source, high energy and fast accumulation by lithologic description, thin section, scanning electron microscope, X-ray diffraction and cathode luminescence in study area (well L13-2-1), neighboring oilfield (well F13-1-1 and F13-1-9) and the east part of C-depression (well H19-1-1, H23-2-1 and H19-2-1). Evidence from lithologic description, mineral identification of thin section, scanning electron microscope, X-ray diffraction and cathode luminescence in the Enping and Zhuhai formations show that sand reservoirs are low composition maturity and low structure maturity (Gen, 2009; Zhang, 1983), and its sediment backgrounds are near source, high energy and fast accumulation. The Enping (E2e) Formation is lake delta facies combined with lake facies.

The Zhuhai (E3z) Formation was formed in alternating depositional environments of delta and tidal flat facies, deeper than 2,500m. The physical properties and oil-bearing property of these two formations are 19-9% and 17-7% for average porosity, 10-100 md and 1-40 md for average permeability, 8-38% and 10-32% for average clay content. Average resistance and oil saturation for oil layer, oil-water layer and water layer are $R > 3.5 \Omega \cdot m$, $S_o > 63\%$, $R: 3.2-1.7 \Omega \cdot m$, $S_o > 45\%$, $R < 2.2 \Omega \cdot m$. These two formations are low-middle porosity, low-middle permeability, high clay content, wide range of oil saturation, and low-middle sand reservoirs. Scanning electron microscope images show that pore spaces are filled by illite, mixture of illite and smectite, kaolinite, smectite and chlorite, some of which are intergranular chemical deposition; some are converted from mud matrix, product of recrystallization and feldspar clayzation (dissolution and alteration). Most of authigenic clay minerals are formed in early-middle diagenesis.

Superiority minerals are illite with relatively low illite/smectite, kaolinite, smectite and chlorite. The shapes of illite and illite/smectite are roll sheet, scale-like, leaf-shaped, sheet and strip wire, and these minerals grew along the margin of particles and formed clay coat (coat thickness: 0.3-1.5 μm). We can clearly see that feldspar clayzation (authigenic clay minerals wrap around the residual feldspar), quartz overgrowth and minerals interchange. The general micro characteristics are intergranular solution pores, intragranular solution pores and mold pores in sand reservoirs of the Enping and Zhuhai formations ([Figure 3](#)). The above characteristics are factors of low resistivity reservoirs.

Detection Methods of Low Resistivity Reservoirs

There are many methods to detect low resistivity reservoirs, such as analysis of geological logging, movable water interpretation of log data, nuclear magnetic resonance technology, overlap of RLLD and AC, dual porosity overlap, rock electricity experiment and thin layers evaluation. In study area, because of incomplete log data and insensitivity of conventional well logs to low resistivity reservoirs, GR spectrum logging technology is taken since it is an effective way of estimation of clay content and identification of clay mineral types (Wu et al, 2008). GR spectrum logging technology can provide not only total amount of GR but also the contents of non-uranium gamma and uranium, thorium and

potassium in rock. The total magnitude of natural radioactivity in rock increases with clay content, and different types of clay minerals have different contents of uranium, thorium and potassium. Through cross-plot and histogram of uranium, thorium and potassium, one can identify the types of clay minerals and estimate relative mass percentage of minerals to interpret reservoirs with the integrated information. [Figure 4](#) and [Figure 5](#) show the cross-plot, types of clay minerals, histogram of mass percentage and statistic analysis of thorium and potassium in well L13-2-1 and well F13-1-1 of Zhuhai and Enping Formations. illite, illite/ smectite , mica can be seen in Zhuhai Formation of both wells, and illite content is high, while there are some feldspar in well L13-2-1; plenty of illite and illite/smectite can be seen in En-ping Formation of both wells, and there are some smectite and kaolinite in well L13-2-1, but there few feldspar. [Figure 5](#) shows the histogram of types of minerals and mass percentage in [Figure 4](#) more straightforwardly and more subtly. Illite is of high mass percentage and stable (9.8-17.7); content of illite/smectite is less and vary widely (1.2-11.9); contents of smectite and kaolinite are low (<1%); the results are consistent with scanning electron microscope characteristics in previous section. In [Table 1](#), residual feldspars are the residual content of feldspar after alteration ([Figure 3f](#)). In study area, the integrated information of stable and single supply, the depth of a formation is stable, the area ratio of alteration feldspar to total feldspar is 30%, shows the total content of feldspar and the alteration feldspar are both high. The less residual feldspars and the more mass percentage of illite and illite/smectite , the more feldspar were clayzated in diagenesis, and the more water saturation were formed in the porosity of sandstone. It is more possible to form conductive water membrane by authigenic illite and illite/smectite around grain than by intergranular clay minerals (lay matrix and their alternative products). Therefore, there is a more chance to be low resistivity for Enping Formation than Zhuhai Formation in well L13-2-1, and for Zhuhai Formation than Enping Formation in well F13-1-1. The reason of high content of feldspar and low residual feldspar and low illite/smectite in Enping Formation of F13-1-1 is that the total amount of alteration feldspar is little or low clayzation of feldspar in diagenesis (Wang et al, 2010).

Mechanism of Lowering Resistivity for Clay Minerals

Based on reservoirs characteristics of the Enping and Zhuhai formation sandstones and the identification results of clay minerals by GR spectrum, clastic reservoirs of the study area are low composition maturity and low structure maturity, higher content of clay and fast accumulation, and its sediment backgrounds are delta and tidal flat. While fast accumulation, matrix clay in intergranular pores gradually change into clay mineral in the process of diagenesis and recrystallization. The minerals, such as a few autogenic mineral (cement), dissolvable K-feldspar and microcline, turn into authigenic illite and illite/smectite. The shapes of illite, illite/ smectite are thin film, sheet and flocculent, which grew around the grains of quartz and feldspar and filled into intergranular pores. These minerals can take negative effect on properties of reservoirs, but they can form plenty of dissolution pores, secondary micropores and micro honeycomb pores. In addition, these authigenic-minerals (illite and mixture of illite/smectite) of water-sensitive, strong ion exchange capacity and alignment are strongly able to absorb water, and then change the water statement. Water molecules absorbed around grains form a complete clay conductive network, and improve the conductivity of formation to lead to low resistivity of reservoirs, so those formations are falsely interpreted as high water saturation and low oil saturation in conventional logging (Zhang et al, 2004). By contrast, other types of clay minerals, such as kaolinite, chlorite and mica are low ion exchange capacity and poor water absorption. When the clays in sandstone porosity are scattered in spots, fiber, uneven clumps, or growth along the grain, or low clayzation and weak recrystallization of mud in diagenesis, despite the content is not low, it is difficult to form a contiguous conductive water network, so there is no effect on the resistivity. [Figure 6](#) is new section of well L13-2-1 after reprocessing and reinterpretation by adding constrains of clay minerals in conventional logging interpretation. There are two low resistivity reservoirs, one oil-water layer and three water-oil layers in Enping: 2,879.5-2,885m (3:low resistivity reservoirs, oil-water layer before, rich oil layer by cores),

2,921-2,927m (4:low resistivity reservoirs, verified by geological logging), 2,951-2,958m (5:oil-water layer), 3,059-3,079m (6:water-oil layer, fluorescent display), 3,088-3,104m (7:water-oil layer, fluorescent display), 3,109-3,139m (8:water-oil layer, fluorescent display); One low resistivity reservoir in Zhuhai: 2,722-2,726m (2:thin rich oil layer by geological logging); One high resistivity reservoir in Zhujiang Formation: 2,494-2,510m (1:thick rich oil layer developed by the oilfield).

Conclusions

It is a great challenge to detect low resistivity reservoirs using conventional logging and logging interpretation standard. It is an effective way to utilize cross-plot and histogram of TH and K in the gamma ray spectrometry logs to identify low resistivity reservoirs of the Enping and Zhuhai formations by estimating clay mineral types and mass percentage. Combined with diagenetic background, micro-geological characteristics, physical properties and oil saturation, a reasonable explanation is made for mechanism of low resistivity. Such analysis can not only avoid missing the real oil formations for logging interpretation, but also give a guide to the research on Paleogene deep reservoirs.

Acknowledgments

We thank the South Oilfield Company in China for providing the data and research grants.

References Cited

- Fu, Wanjun, 2000, Influence of clay minerals on sandstone reservoir properties: Journal of Palaeogeography, v. 2/3, p. 58-67.
- Geng, Wei, 2009, Characteristics of Reservoir Sedimentology of Paleogene in Huizhou Depression, Zhujiangkou Basin: Chengdu University of Technology Master's thesis.
- Hu, Xiang-yang, Wu Hong-shen, Gao Hua, and Wang Li, 2010, Study of reservoir parameters in Logging area of oil and gas filed in Pearl River Mouth Basin: Journal of Oil and Gas Technology, v. 32/5, p. 16-20.
- Liao, Ming-guang, Chong-hua Su, Hong Tang, De-hui Tan, Wei Jiang, and Xiao-qiang Chen, 2010, Geological Genesis of Low Resistivity Formation with Thin Sand-Shale Interlayer - An example from M1 oil measure of a reservoir in Pearl River Mouth basin: Xinjing Petroleum Geology, v. 25/2, p. 154-157.
- Wang, Ruili, Sun Wanhua, Zou Mingsheng, Liu Mingquan, and Yang Xibing, 2010, Analysis on cause of low-resistivity oil layer formation in Weixinan Sag of Beibuwan Basin, Fault-Block: Oil & Gas field, v. 17/5, p. 642-645.
- Wu, Chun-wen, Zhao Wen-jie, and Bai Qiang, 2005, Application of Natural Gamma Ray Spectrometry Logging in Glutenite Reservoir: Well Logging Technology, v. 29/1, p. 46-48.

Zhang, Li-xia, Zhu Guo-hua, and Li Min, 2004, Origin of Cretaceous Low-resistivity Reservoirs in Junggar Basin: Xinjing Petroleum Geology, v. 25/4, p. 388-389.

Zhang, Tiangang, 1983, Electronic scanning microscopic examination of clay minerals in sandstones: Journal of Mineralogy and Petrology, v. 4/1, p. 35-39.

Zou, Xinbo and Wei Congda, 2007, Origin and distribution of remaining oil in sandstone oil reservoir at extra-high water cut stage with the transitional facies sandstone oil reservoir—taking Lufeng 13-1 Oilfield, Pearl Mouth Basin as an example: PGRE, v. 14/6, p. 97-99.

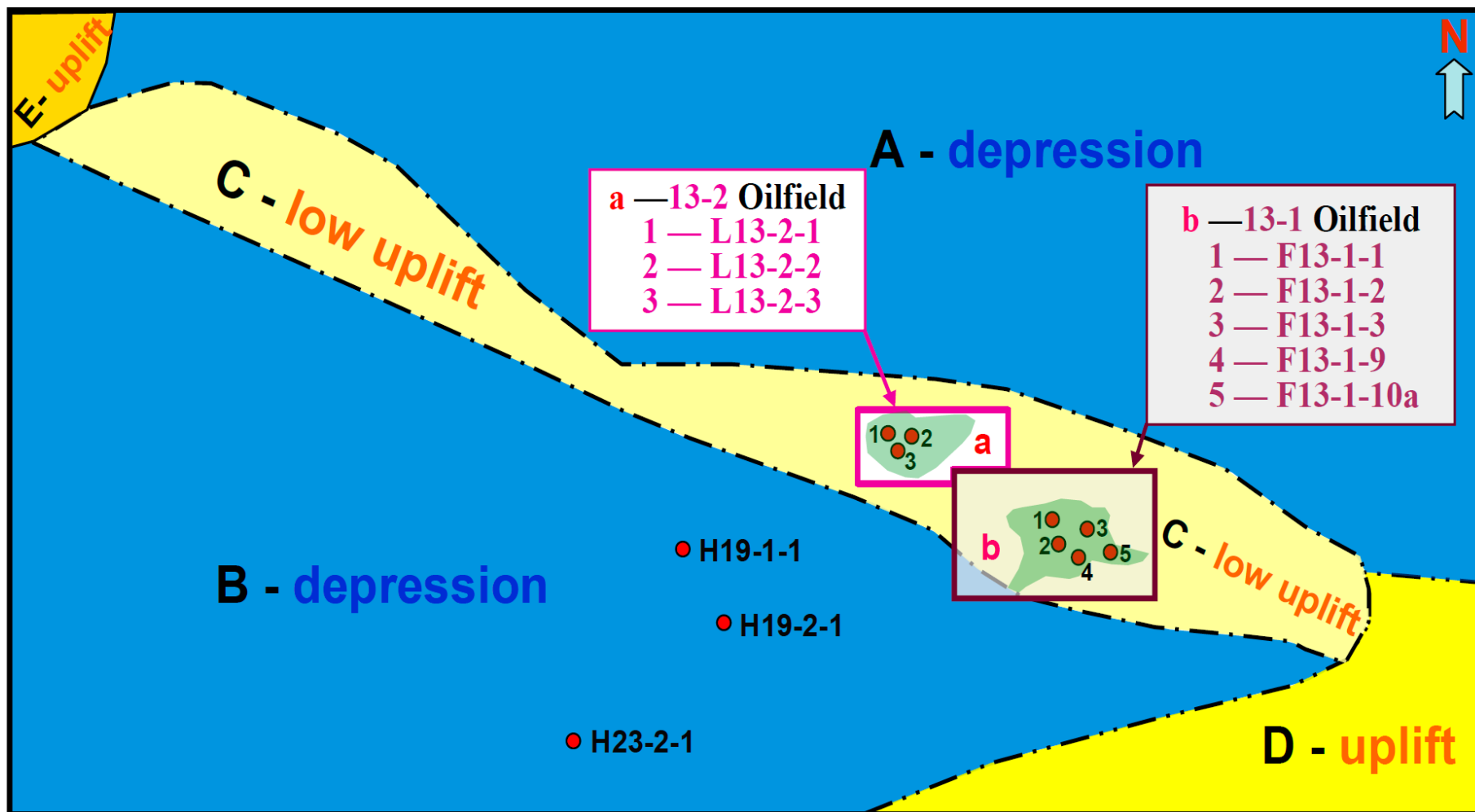


Figure 1. a-13-2 Oilfield (study area), b-13-1 oilfield and east part of B depression of X basin in south China.

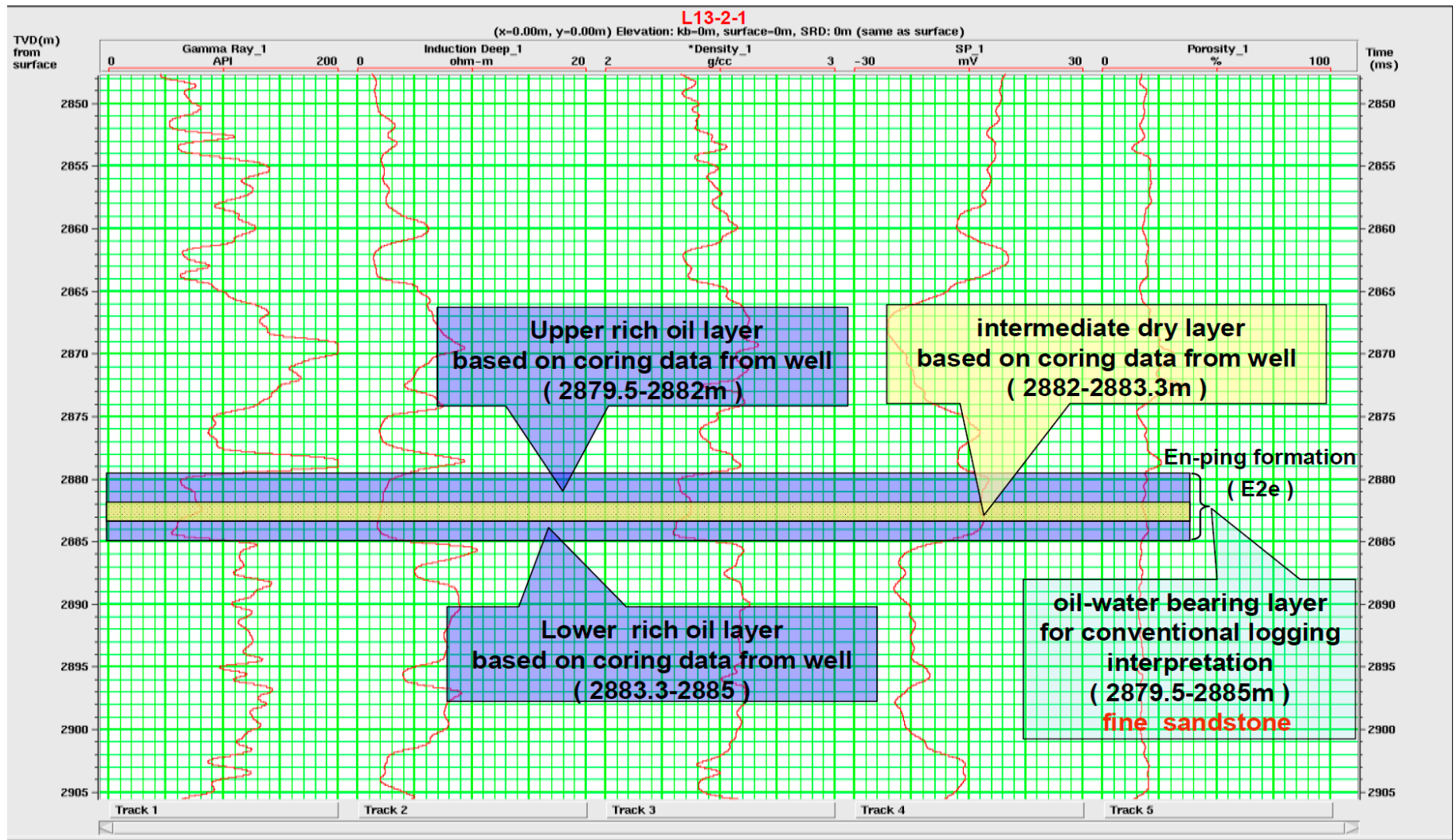


Figure 2. Low resistivity characteristics on well L13-2-1 in a-13-2 Oilfield (study area).

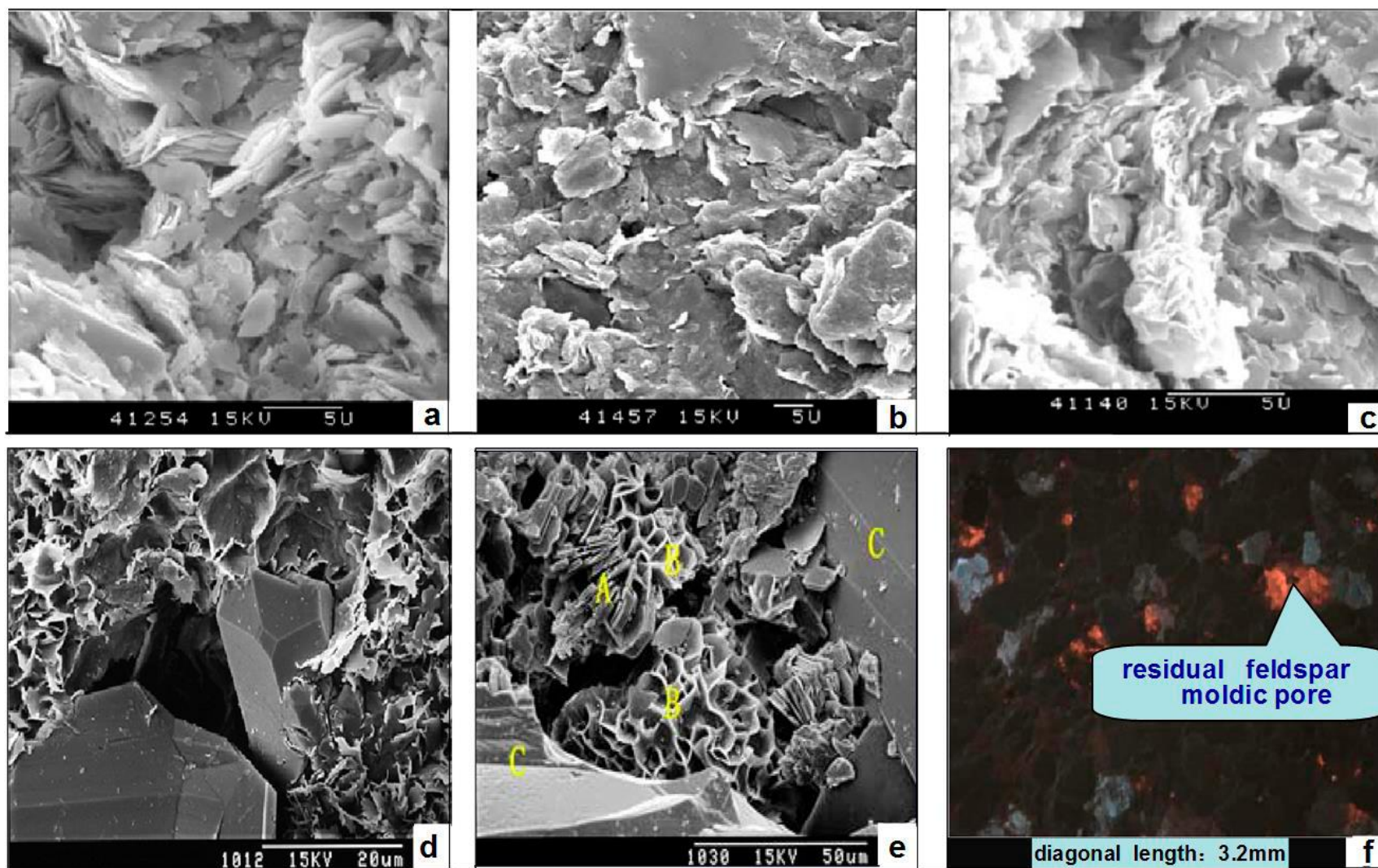


Figure 3. Scanning electron microscope characteristics of sand samples in Paleogene formation of B-depression. (a) Recrystallization ledikite in intergranular pores, 3,220m, well H23-2-1 of Zhuhai formation, (b) mixture of ledikite and surface and pores on surface of scrap grain (feldspar and quartz), 3,323.8m, well H23-2-1 of Zhu-hai formation, (c) intergranular sheet ledikite and pores, 3,407m, well H23-2-1 of Zhuhai formation, (d) authigenic clay minerals and scales-like ledikite in early-middle of diagenesis, 3913.1m, well H19-1-1 of Zhuhai formation, (e) intergranular kaolinite-ledikite interchange in early diagenesis (kaolinite-A, Illite-B, quartz overgrowth-C), 3,687.7m, well H19-2-1 of Enping formation, (f) cathodeluminescence sections of non-clayzation feldspar (bright blue-gray) and micritization feldspar (dark brown), quartz and mold are non-luminous, 3,548.5m, well H19-2-1 of Enping formation.

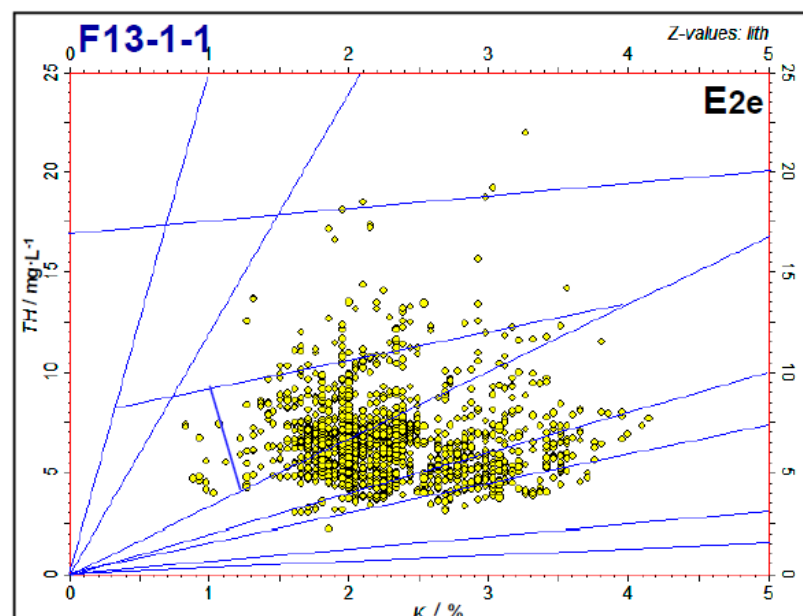
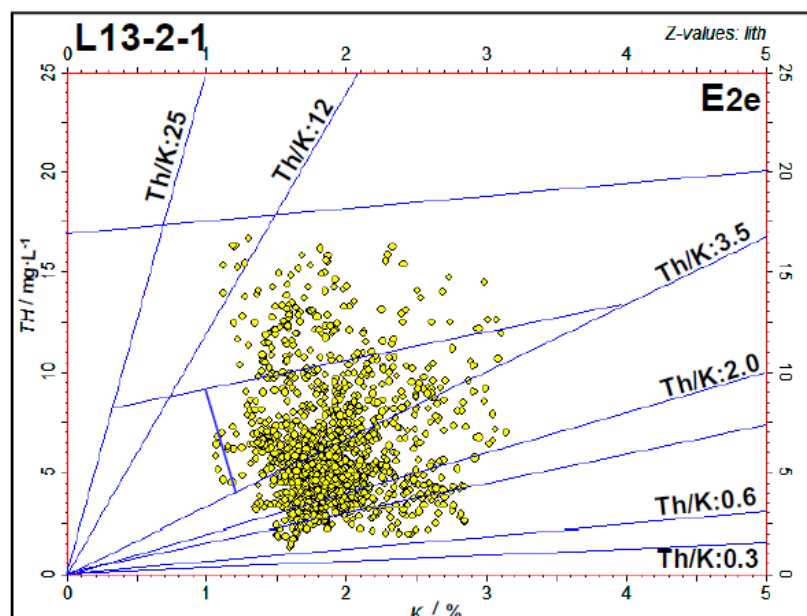
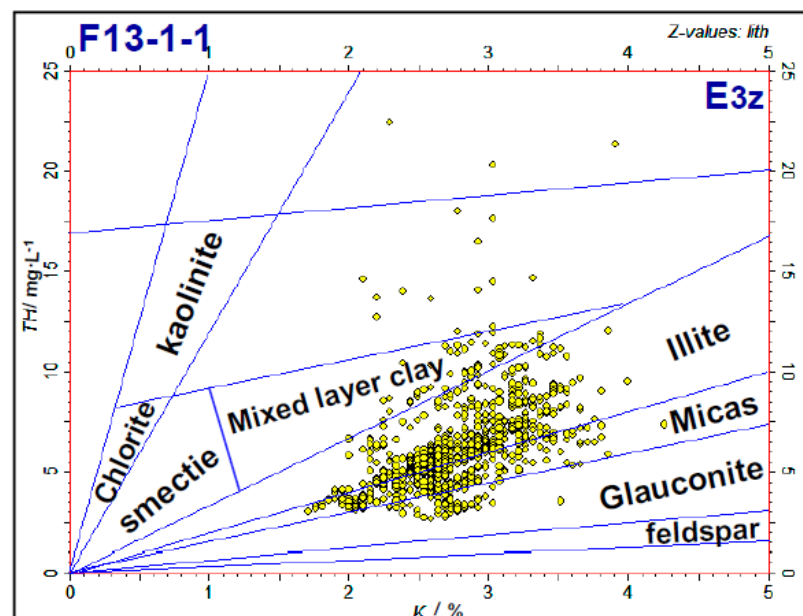
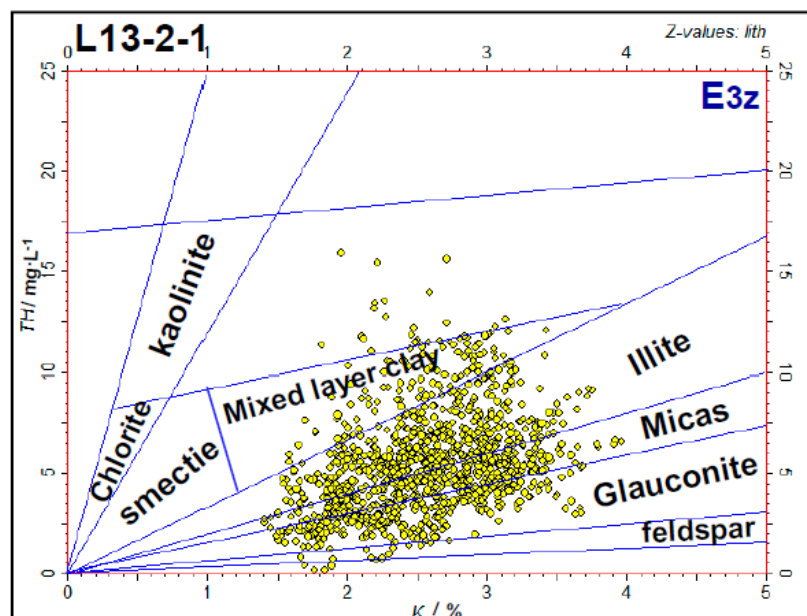


Figure 4. The cross-plot of thorium and potassium in Zhuhai and Enping Formations of well L13-2-1 and well F13-1-1. Mold is non-luminous, 3,548.5m, well H19-2-1 of Enping formation.

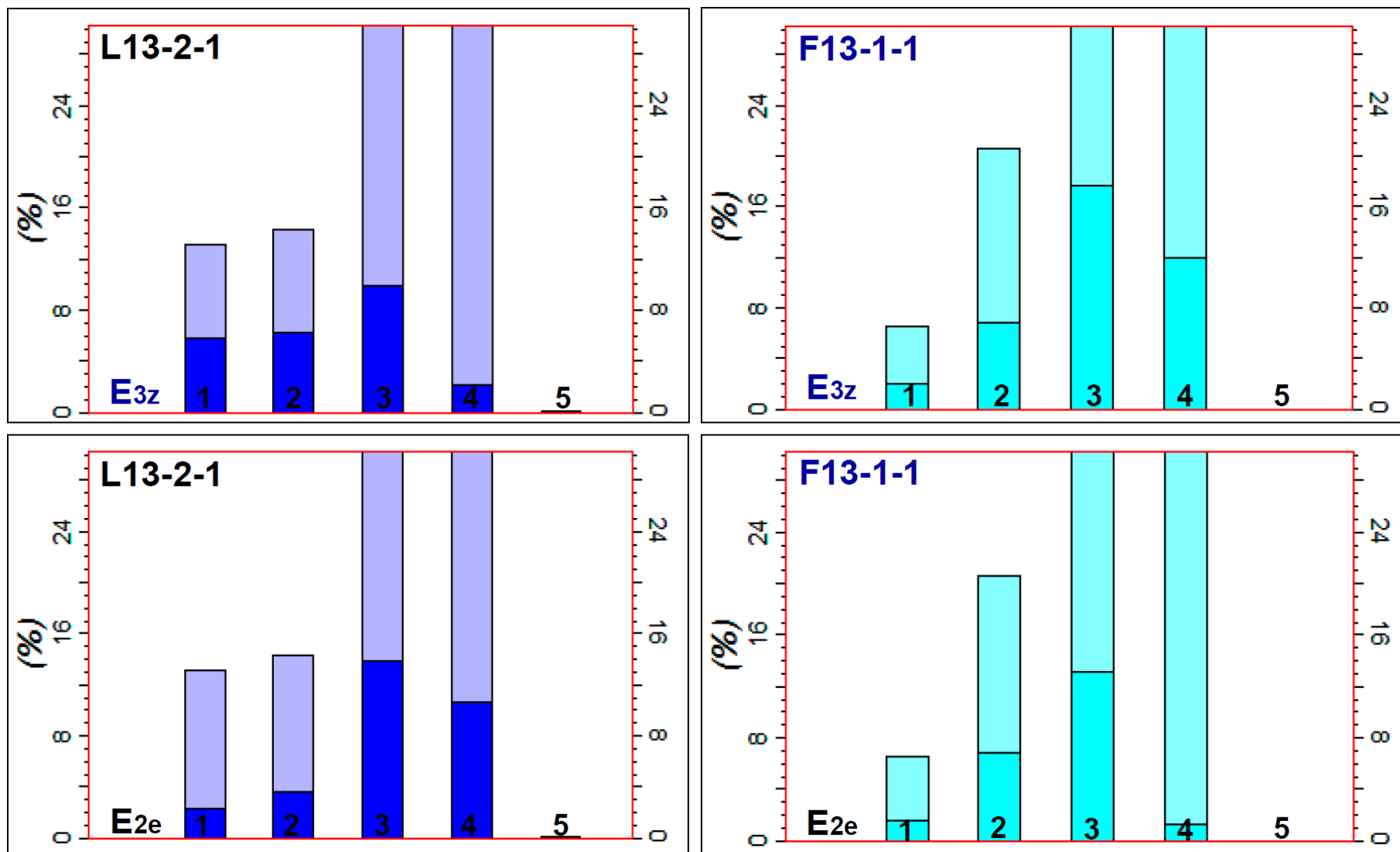


Figure 5. The histogram of types of minerals and mass percentage of deep sandstone in well L13-2-1 and well F13-1-1. 1-residual feldspar; 2-micas; 3-illite; 4-illite/smectite mixed layer clay; 5-smectite. E3z: Zhuhai Formation, Oligocene, Paleogene; E2e: Enping Formation, Oligocene, Paleogene.

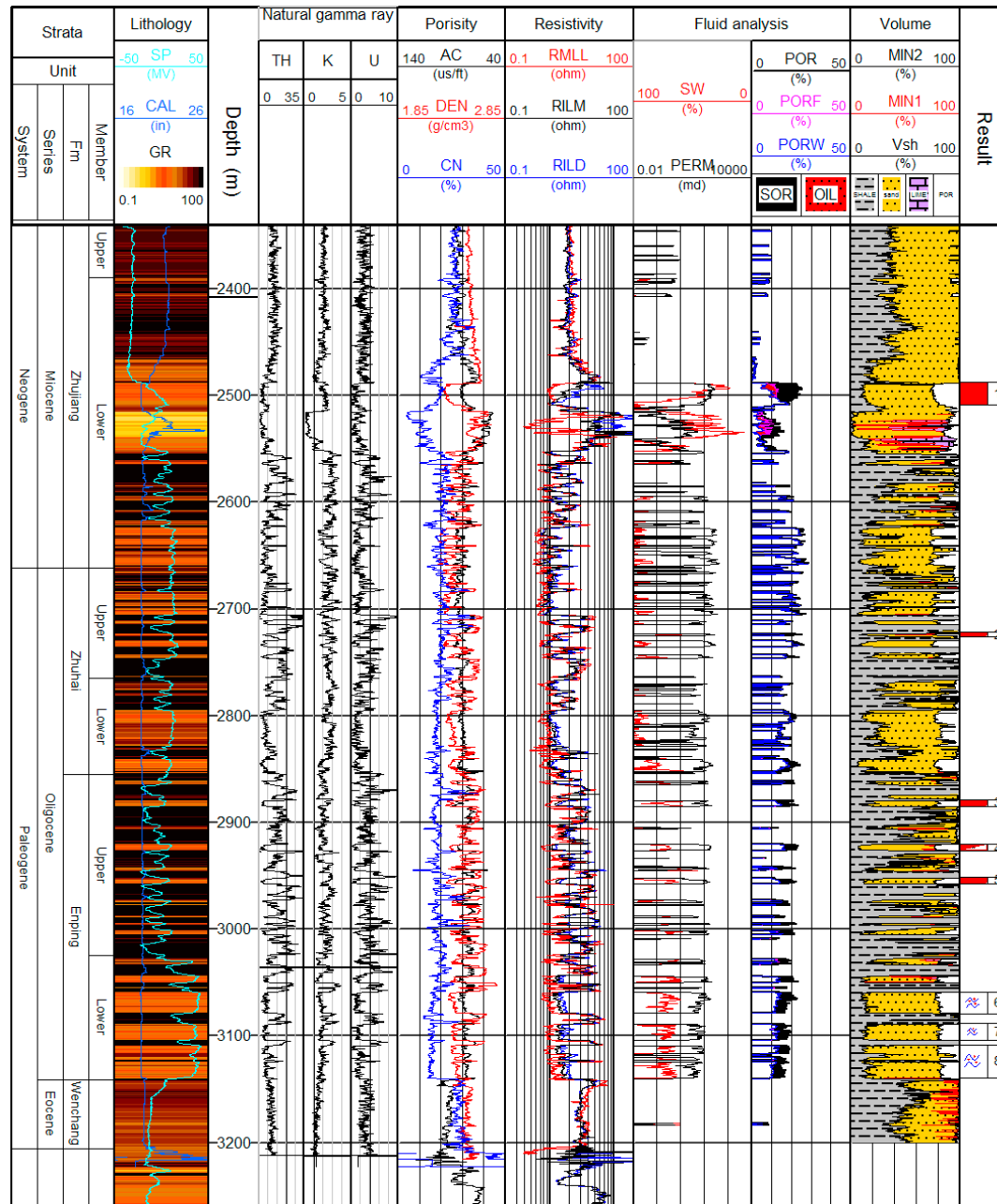


Figure 6. New interpretation results of deep oil-water layer in well L13-2-1.

Paleogene	item well name	main clay mineral types and mass percentage(%)			mass percentate of residual feldspar (%)	average percentate of stastic feldspar	degree of feldspar clayzation
		Illite	Illite/smectite	Illite + Illite/smectite			
E3z	L13-2-1	9.8	2.05	11.85	6.9	16.0%	weak
	F13-1-1	17.7	11.9	29.6	2.0		strong
E2e	L13-2-1	13.8	10.6	24.4	2.15	23.4%	weak
	F13-1-1	13	1.2	14.2	1.5		middle

Table 1. Statistics of clay minerals types, crap feldspar and mass percentage in well L13-2-1 and well F13-1-1.